Published in final edited form as:
Dev Cell. 2014 October 13; 31(1): 114–127. doi:10.1016/j.devcel.2014.07.027.

Combining Genetic Perturbations and Proteomics to Examine Kinase-Phosphatase Networks in *Drosophila* Embryos

Richelle Sopko[1,*], **Marianna Foos**[1,3], **Arunachalam Vinayagam**[1], **Bo Zhai**[2,4], **Richard Binari**[1], **Yanhui Hu**[1], **Sakara Randklev**[1], **Lizabeth A. Perkins**[1], **Steven P. Gygi**[2], and **Norbert Perrimon**[1,3,*]

[1]Department of Genetics, Harvard Medical School, Boston MA 02115 USA

[2]Department of Cell Biology, Harvard Medical School, Boston MA 02115 USA

[3]Howard Hughes Medical Institute, Boston MA 02115 USA

Summary

Connecting phosphorylation events to kinases and phosphatases is key to understanding the molecular organization and signaling dynamics of networks. We have generated a validated set of transgenic RNA-interference reagents for knockdown and characterization of all protein kinases and phosphatases present during early *Drosophila melanogaster* development. These genetic tools enable collection of sufficient quantities of embryos depleted of single gene products for proteomics. As a demonstration of an application of the collection, we have used multiplexed isobaric-labeling for quantitative proteomics to derive global phosphorylation signatures associated with kinase-depleted embryos, in order to systematically link phosphosites with relevant kinases. We demonstrate how this strategy uncovers kinase consensus motifs and prioritizes phosphoproteins for kinase target validation. We validate this approach by providing auxiliary evidence for Wee kinase-directed regulation of the chromatin regulator Stonewall. Further, we show how correlative phosphorylation at the site level can indicate function, as exemplified by Sterile20-like kinase-dependent regulation of Stat92E.

Introduction

Despite the ease with which we can identify protein phosphorylation, in the vast majority of cases the protein kinase(s) or phosphatase(s) responsible for controlling any particular phosphorylation event is unknown. We sought to develop a proteomic strategy to easily and systematically screen for candidate protein kinase and phosphatase substrates in *Drosophila melanogaster* embryos, with the goal of identifying specific residues these enzymes target in

[*]Correspondence: rsopko@genetics.med.harvard.edu, perrimon@receptor.med.harvard.edu.
[4]current address: St. Jude Children's Research Hospital, Memphis TN 38105 USA

Supplemental Data
Supplemental Data includes Extended Experimental Procedures (including all experimental and computational methods), six figures, and seven tables. A detailed Protocol for mass spectrometric sample preparation is provided in a separate PDF.

the context of development. *D. melanogaster* is an ideal model for the dissection of signaling mechanisms, as the majority of transcription in the embryo occurs after the mid-blastula transition (MBT), and thus transcriptional feedback has relatively no impact on the phosphoproteome in early embryos. Additionally, since the embryo is a syncytium prior to cellularization at the MBT, distortions in phosphosite measurements due to contributions from multiple cell types can be avoided. However, acquiring sufficient material from mutant embryos for proteomic studies is a challenge. The classical technique to generate maternally-deficient embryos, relying on the production of germline clones using the FLP recombinase-mediated dominant female sterile technique (Chou and Perrimon, 1996), is labor intensive as it involves the construction of complex genotypes. Moreover, background mutations on the FRT-bearing chromosome can confound phenotype interpretation and the approach does not typically yield enough material for proteomic studies.

Here we describe how we have used genetic manipulation by transgenic RNA interference (RNAi) to derive sufficient quantities of embryos for phosphoproteomic analyses. RNAi is a well-founded method to analyze gene function in *D. melanogaster* (Perrimon et al., 2010), but the efficacy of RNAi during early embryogenesis has only recently been improved to enable robust gene knockdown during this developmental stage (Ni et al., 2011). By employing the Gal4/UAS system (Brand and Perrimon, 1993) to temporally and spatially restrict expression of RNAi reagents, we confined protein kinase and phosphatase knockdown specifically to the germline. Using this strategy we were able to query maternal gene function without impacting viability of the animal, since an intact germline is dispensable for organismal development. We generated and validated a transgenic RNAi library that targets all protein kinases and phosphatases expressed in the *D. melanogaster* germline. Through rigorous characterization of our collection we uncovered new maternal effect genes, and verified previously implicated kinases and phosphatases in early *D. melanogaster* development. Further, we systematically monitored global phosphoproteome alterations in kinase-deficient embryos for the purpose of illustrating how the method can generate lists of candidate kinase substrates. The approach illuminated kinase-dependent signaling and permitted the unbiased prediction of kinase consensus motifs that match kinase specificities previously characterized *in vitro.* As anticipated, the strategy identified downregulated phosphoproteins that include *bona fide* kinase substrates of the depleted kinase and an extensive list of candidate kinase targeted substrates and phosphosites. We further establish that two phosphosites consistently responding in the same direction (positive correlation) or the opposite direction (negative correlation) in different genetic contexts can illuminate phosphosite functionality. Given the extensive similarity between human and *D. melanogaster* kinases, and the conservation of functional phosphorylation (Gnad et al., 2010; Landry et al., 2009), we anticipate that insight gained from our data and analyses will inform future mammalian studies.

Results

Compilation of the maternally inherited protein kinome and phosphatasome

The *D. melanogaster* genome encodes 32 tyrosine kinases, 237 serine/threonine kinases, and 112 protein phosphatases (Manning et al., 2002; Morrison et al., 2000). To systematically

link protein phosphorylation sites with their cognate kinases and phosphatases in *D. melanogaster* we first identified the complement of kinase and phosphatase mRNAs that are deposited maternally and contribute to the early zygote, by analyzing developmental time course RNA-Seq data (Graveley et al., 2011). Using an RPKM (Reads Per Kilobase of exon model per Million mapped reads) cutoff of 3, determined by comparison to quantitative real time PCR (RT-qPCR) analysis of staged embryos (Hu et al., 2013b), we determined that 201 protein kinase-encoding transcripts and 76 protein phosphatase-encoding transcripts (Figure 1A, Table S1) are present during the first four hours of embryogenesis (stages 1 – 8). This accounts for 75% and 68% of all protein kinases and phosphatases, respectively, encoded in the *D. melanogaster* genome (Figure 1A). We independently verified the presence of these transcripts by RT-qPCR (Figure 2A), but detected only 172 kinases and 67 phosphatases in two-hour old embryos (stages 1 – 4) at the protein level based on peptide MS1 feature intensities from shotgun mass spectrometry (Figure 1A). Most kinases and phosphatases we identified as transcripts were reliably detected as protein. We found that for only 28 kinases and 9 phosphatases where mRNA was identified, the corresponding protein at the appropriate time interval was not detected (Table S1). Thus, mRNA detection was generally a good predictor of protein presence. However, when considering levels rather than identity, we found no correlation between mRNA and protein (Figure S1), similar to observations from large-scale studies in *Schizosaccharomyces pombe* (Marguerat et al., 2012). Using a stringent criterion of conservation (*i.e.* at least three independent prediction tools support an orthologous gene-pair relationship (Hu et al., 2013a)), we found that nearly all protein kinases and phosphatases expressed during early *D. melanogaster* development are conserved to human (Figure 1B and 1C; Table S1). On the contrary, conservation to yeast is far more limited.

Generation and validation of the transgenic shRNA collection targeting kinases and phosphatases

We previously demonstrated the utility of short hairpin RNAs (shRNAs) embedded in an endogenous microRNA scaffold to knockdown maternal gene function in *D. melanogaster* embryos. A side-by-side comparison of shRNA with long dsRNA transgenic lines indicates that screening of shRNA lines triples the frequency of RNAi-derived germline phenotypes, (Yan et al., 2014) generally due to higher expression of shRNAs in the germline (Ni et al., 2011). Having characterized the requirements for efficient gene knockdown during oogenesis, we sought to generate a complete and validated set of shRNA-expressing transgenic lines capable of targeting protein kinases and phosphatases contributed maternally to the developing embryo. To induce shRNA expression specifically in the female germline using the Gal4-UAS system, we crossed females heterozygous for a UAS-shRNA and either MTD-Gal4 (a line bearing three copies of Gal4 expressed sequentially throughout oogenesis (Petrella et al., 2007)) or tub-Gal4 (a line bearing two insertions of Gal4 expressed from a maternal tubulin promoter during mid and late oogenesis (Staller et al., 2013)), to shRNA-bearing males in order to recover fertilized eggs. We analyzed more than 450 transgenic lines expressing shRNAs targeting protein kinases and phosphatases (Table S2). We were unable to recover eggs from ~12% of the lines crossed to MTD-Gal4, accounting for 46 kinases and 6 phosphatases, implying that these genes are required for early oogenesis.

For those lines from which we could recover eggs, we determined by RT-qPCR following the Minimum Information for Publication of Quantitative Real-Time PCR Experiments (MIQE) guidelines (Bustin et al., 2009) that more than half of the ~450 transgenic lines we analyzed generated greater than 60% knockdown of corresponding kinase or phosphatase mRNA levels in 0–4 hour embryos, relative to a control shRNA targeting EGFP (Figure 2A and Figure S2A). We observed excellent correlation between knockdown at the mRNA and protein level, which was assessed by comparing mRNA levels assessed by RT-qPCR to immunoblots of a subset of proteins for which antibodies were available (Figure 2B). We were interested to determine the number of transgenic lines that would need to be considered to observe at least one achieving >60% knockdown of the targeted transcript. We found that when considering two unique shRNAs targeting the same gene product, this occurs at a frequency of 86% (N=81 pairs) (Figure S2B). This data suggests that generating two independent shRNA lines is usually sufficient for obtaining at least one line that confers adequate knockdown. Interestingly, many cases of poor knockdown can be attributed to shRNA targeting design. Specifically, our data indicate that shRNAs targeting the transcript coding sequence (CDS) are more effective at knockdown than those targeting 3′UTRs (Figure S2C), possibly reflecting inaccuracies in UTR annotation (Hu et al., 2013b).

Notably, we found no correlation between the degree of knockdown and the level of corresponding transcript in untreated early embryos (Figure S2D). Further, our data exhibit no bias towards the concentration of recovered RNA or the date of sample collection (Figure S2E and S2F). Taken together, our collection consists of at least one transgenic line that provides a minimum of 60% knockdown for each maternally inherited protein kinase and phosphatase.

Assessment of transgenic shRNA collection phenotypes

Our shRNA-directed knockdown strategy recapitulated many documented maternal effect phenotypes (Figure 3A). As expected we observed anterior-posterior terminal defects following the disruption of terminal signaling, such as that resulting from knockdown of the receptor tyrosine kinase *torso*, the SHP2 phosphatase ortholog *corkscrew*, or the downstream kinase suppressor of ras, *ksr* (Figure 3A). Altogether we observed maternal effect phenotypes for ~18% of lines that achieved 60% or greater knockdown (Figure 3B and Table S2), representing approximately 33% and 18% respectively of protein kinases and phosphatases expressed during early embryogenesis. Of those protein kinases and phosphatases for which a maternal effect phenotype has been reported, we observed the same qualitative phenotype as that described in the literature approximately 74% of the time (26/35 genes considering germline clone-derived embryos, 2/3 considering embryos derived from homozygous mutant mothers; Table S3A). Anomalies can likely be attributed to: 1) weak hypomorphic alleles generating a less severe phenotype than extensive knockdown; 2) insufficient knockdown by an shRNA to produce phenotypes generated by strong or null mutant alleles; or 3) in the case of embryos derived from mutant mothers, an effect resulting from mutant somatic follicular cells. Despite the fact that protein kinases and phosphatases are among the best-characterized classes of genes, we uncovered unappreciated phenotypes for approximately 40 of these enzymes, implying previously unrecognized roles in oogenesis and early embryogenesis. Further, knockdown of an additional 12 predicted

kinases and phosphatases resulted in oogenesis and maternal-effect phenotypes, warranting more extensive characterization. A searchable interface to query genes for individual transgenic lines, a description of their knockdown and embryonic phenotypes, and photos of cuticle preparations for those with maternal effect phenotypes can be found at http://www.flyrnai.org/RSVP.html.

We addressed the possibility and frequency of shRNAs generating phenotypes as a result of off-target effects (OTEs) in two ways. First, we compared pairs of unique shRNAs targeting the same gene for similar phenotypes. Comparing twenty-four efficient targeting pairs, we found that 80% produced the same qualitative phenotype (Figure 3C; Table S3B). Four of the six cases of a differential phenotype can be explained by the extent of knockdown. Second, we established transgenic lines expressing 'C911' versions of a targeting shRNA: a near identical shRNA but with complementary nucleotides situated at positions 9–11. The mismatched shRNA precludes on-target binding while maintaining off-target binding since anti-sense and sense seed sequences remain intact (Buehler et al., 2012). Consistent with phenotypes resulting from on-targeting specificity provided by perfect complementary of the shRNA, we eliminated phenotypes resulting from expression of sixteen unique shRNAs, by mutating the central three nucleotides of the shRNA. We verified by RT-qPCR that mutation of these three residues eliminated knockdown of corresponding kinase transcripts the shRNA originally targeted (data not shown). Thus, we conclude that the prevalence of OTEs impacting early embryogenesis is minimal with the shRNA targeting strategy.

A resource providing accessibility for proteomic analyses and kinase characterization

Our current reagents for germline-specific RNAi make it relatively easy to obtain large numbers of eggs depleted of a single gene product. This allowed us to perform quantitative proteomic experiments to measure the global effect of each perturbation on the phosphoproteome (Figure 4A). We anticipated that a relative quantitative and global assessment of altered phosphorylation in protein kinase-deficient embryonic extracts could provide a list of putative protein kinase-substrate and phosphosite matches. We also reasoned that phosphorylation signatures could also be used to predict roles for protein kinases and phosphatases in specific biological processes, and reveal functional redundancy.

We initially assessed the reproducibility of phosphoproteomic profiles generated from analysis of separate populations of control shRNA embryos. We utilized mass spectrometry and an isobaric labeling strategy (see Protocol) that enables multiplexing and relative quantification between samples (see Extended Experimental Procedures). Since ~700 embryos constitute the amount of material (~1mg protein) we chemically label, the phosphoproteomic profile is a representative average of phosphorylation in this population. Amine reactive TMT Isobaric Mass Tags, identical in mass but differing in their isotopic distribution of atoms, permits the simultaneous spectral identification of unique reporter ions generated from MS2-based fragmentation of each tag from labeled peptides. We compared TMT reporter ion intensities and phosphopeptide identities from three TMT-labeled control shRNA embryo populations in two independent experiments (Table S4). When considering those phosphopeptides in the same multiplex experiment (10,166 phosphopeptides for one experiment and 8,032 for the other; see Supplemental Experimental Procedures for

normalization and specific criteria), we generally identify the same phosphopeptide in all three biological replicates (~99% of the time). In the two independent experiments we observed phosphopeptide levels deviating an average of 7% (Figure S3A) and 29% (Figure S3B) between three biological replicates. This indicates that variability in factors such as peptide labeling and embryo collection have little influence on our ability to consistently detect the majority of phosphopeptides.

Given the reproducibility between control shRNA replicates, we extended our phosphoproteomic examination to embryos derived from females expressing efficient shRNAs (as determined by RT-qPCR) targeting nineteen different protein kinases (Figure 4B). We were able to quantify nearly 8500 unique phosphosites among nineteen deficient kinase samples (Table S5A–D). The number of unique phosphosites we quantified between experiments, ranging from 6,331 to 2,448, was based on the number of unique phosphopeptides identified per experiment, ranging from between 22,942 and 12,201. Notably, 1,140 phosphosites were quantified in all nineteen kinase knockdown conditions, 1,343 in ten kinase knockdown conditions, and 4,358 in five kinase knockdown conditions. The majority of phosphopeptides in each kinase-deficient sample were unchanging in abundance relative to the same control shRNA included in each multiplex experiment. In terms of candidate kinase-targeted phosphosites, either direct or indirect, we consider those downregulated sites with changes of 1.5-fold or greater in kinase-deficient embryos relative to control embryos, since observed phosphopeptides for seven shRNA-targeted kinases (Wee, Tao, Atg1, Gilgamesh (Gish), Lkb1, Grapes (Grp), and Sterile20-like kinase (Slik)) minimally met this criterion (2.27-fold, 1.95-fold, 1.69-fold, 2.24-fold, 2.68-fold, 1.98-fold, and 2.1-fold respectively) in corresponding kinase-deficient embryos (Figure S4A). We did not detect phosphopeptides for the other twelve shRNA-targeted kinases. Moreover, changes in known substrates of shRNA-targeted kinases, for instance Histone H3, Med13 and Stat92E in *Cdk8* deficient embryos (downregulated 2.2-fold, 1.8-fold and 2.4-fold respectively), and Cdk1, Klp61F and Hsp83 (downregulated 1.4-fold, 2.1-fold, and 1.7-fold respectively) in *wee* deficient embryos, approach this value. Indeed, for a third of the *D. melanogaster* orthologs of literature curated Cdk8 substrates in yeast (Sharifpoor et al., 2011) we identified, one or more respective phosphopeptides were downregulated >1.5 fold in *Cdk8* deficient embryos (Table S5E). Using this criterion, the number of downregulated phosphosites in kinase-deficient profiles ranged from 22 (*Bub1* deficient embryos) to 752 (*Cdk8* deficient embryos) (Table S5). Of note, while our *Bub1* targeting-shRNA generated efficient knockdown (99% knockdown), *Bub1*-deficient embryos exhibited no morphological or hatch rate defects (Table S2), consistent with minimal effects on the phosphoproteome. Conversely, knockdown of *Cdk8*, a cyclin-dependent kinase influencing transcription and cell cycle progression (Szilagyi and Gustafsson, 2013), resulted in dramatic and penetrant morphological and hatch rate phenotypes, consistent with extensive modulation of the observed phosphoproteome. We speculate that among those phosphosites downregulated >1.5-fold in the nineteen kinase-deficient contexts we surveyed are sites directly targeted by the corresponding depleted kinase(s), as well as indirect targets altered downstream of the manipulated kinase. For instance, in the case of *gish*-deficient embryos, we observed enrichment of downregulated phosphorylation of proteins involved in Hedgehog (Hh) and Wnt/Wingless (Wg) pathways (Table S5B), consistent with a role for

Gish in mediating Hh and Wg signaling (Davidson et al., 2005; Hummel et al., 2002). These data indicate that by monitoring changes in the phosphoproteome one can effectively screen for candidate substrates and alterations in signaling downstream of the targeted kinase. However, further scrutiny of any altered phosphosite is required to prove a kinase-substrate relationship, as we demonstrate below.

In order to distinguish genuine kinase targets from phosphosite alterations due to protein instability, we classified phosphoproteins with two or more downregulated phosphosites (> 1.5-fold) into five categories based on the directionality of change of the majority of identified phosphosites for each individual protein: Type 1 – the majority of phosphosites do not change; Type 2 – the majority of phosphosites are downregulated; Type 3 - all phosphosites are downregulated; Type 4 - most phosphosites are upregulated; Type 5 – indistinguishable due to an equal distribution of unchanged, upregulated or downregulated phosphosites (Figure 4C). In considering at least two phosphosites we increase the probability that the corresponding phosphoprotein is indeed subjected to degradation and not merely reduced in phosphorylation at a single site. Type 1 and Type 4 phosphoproteins are those for which we can reasonably discount the possibility of protein degradation as a mechanism of downregulated phosphorylation, and thus are considered high priority candidates for phosphorylation by the respective kinase. The observed downregulation of Type 3 phosphoproteins on the other hand, can be explained by indirect mechanisms leading to protein degradation, such as altered protein-protein interactions, or phosphorylation-mediated degradation. Although most phosphoproteins in our dataset are of Type 1 (Figure 4C), Type 3 phosphoproteins account for ~20% on average of those proteins with two or more downregulated phosphosites in each kinase depletion condition. This percentage is in line with previous reports that protein expression changes account for less than 25% of differential phosphorylation (Bodenmiller et al., 2010; Wu et al., 2011). We scrutinized respective transcripts for Type 2 and Type 3 phosphoproteins in order to identify and filter our dataset of potential OTEs due to partial complementarity of the targeting shRNA to unintended transcripts. By comparison to the frequency of partial complementarity of each targeting shRNA (seven nucleotide match to seed) to the early embryonic transcriptome, we find a relatively weak probability for partial complementarity of our targeting shRNAs to 3′ UTRs or transcripts of Type 2 phosphoproteins (see Supplemental data). This probability declines when considering Type 3 phosphoproteins, indicating off-targets are not enriched in our dataset and are therefore unlikely to explain alterations observed in our analyses. To further substantiate this assumption, we proceeded to knockdown respective transcripts for Type 3 phosphoproteins with the best matches to each corresponding kinase shRNA seed. Germline-specific knockdown of ten candidate off-targets predicted for six kinase-targeting shRNAs failed to generate phenotypes that could explain specific phenotypes attributed to the corresponding kinase shRNA (see Supplemental data).

Extracting patterns in phosphorylation datasets to find kinase-substrate (KS) relationships

We speculated that we might be able to extract kinase-substrate relationships and insight into signaling pathway connectivity from our phosphorylation dataset as a whole by examining patterns in phospho-alterations among kinase-deficient contexts. For instance, since most kinases are activated by phosphorylation, correlative phosphorylation events

observed between kinases and other proteins could be indicative of kinase-substrate (KS) relationships. On the other hand, anti-correlative phosphorylation could be additionally informative; inhibitory phosphorylation of a kinase would always be out of phase with phosphorylation of that kinase's respective targets. To explore such possibilities, we surveyed correlations in phosphorylation changes (>1.5-fold cutoff relative to a control shRNA) between identified phosphosite pairs among our kinase-deficient conditions (447,585 correlative pairs involving 2058 phosphosites; Table S6A). When considering phosphosite pairs exhibiting positive or negative correlation in at least four kinase-deficient conditions (25,077 correlative pairs) we find enrichment for authentic KS pairs (Figure 5A), derived from 133,051 *D. melanogaster* KS pairs (Table S6B) predicted from 179 conserved human kinase phosphorylation motifs by NetPhorest (Miller et al., 2008), and from mapping of 517 gold standard KS pairs in yeast (Sharifpoor et al., 2011) to *D. melanogaster*. Enrichment for authentic KS pairs still exists when considering phosphosite pairs correlating in only 2 or 3 kinase-deficient conditions (Figure S5A). Strikingly, we also find enrichment for correlative phosphorylation among components of the same protein complex (p-value: 7.5e–157), further substantiating how this phenomenon can be exploited to identify functionally relevant phosphosites.

While correlative analysis can clearly illuminate direct KS relationships in large-scale phosphorylation data, it can also provide functional information if one has a priori knowledge of the consequence of phosphorylation of one of the participating phosphosites. We exemplify this with the case of Slik and Stat92E. Phosphorylation of the Stat92E transcription factor at Tyr711 promotes DNA binding (Yan et al., 1996). We found that phosphorylation at this particular site positively correlates with phosphorylation of Slik at Ser1376 (Figure 5B), suggestive of a relationship between Slik and Stat92E; the probability of observing two phosphosites correlating among six kinase deficient profiles is rare (p-value: 1.4e–5). We predicted that Slik activates Stat92E given that reduced Stat92E phosphorylation in *slik*-deficient embryos (Figure 5C) cannot be explained by instability of Stat92E protein (Figure S5B). Indeed, Stat92E target gene expression was downregulated in *slik* dsRNA treated cells (Figure 5D). Insulin has been reported to enhance growth hormone-induced Stat activation in mature adipose cells (Zhang et al., 2013) and Stat may be a direct target of the insulin receptor (Sawka-Verhelle et al., 1997). We confirmed an increase in the activating phosphorylation of Stat92E in cells treated with insulin (Figure 5C). Remarkably, we observed that more than a quarter of phosphoproteins downregulated in *slik* deficient embryos are upregulated in cells in response to insulin, including Slik (Figure 5C, Figure S5E–F). Moreover, 30% of phosphoproteins downregulated >1.3-fold in *slik* deficient embryos (Table S7) were found to physically interact with components of the insulin-signaling network (Glatter et al., 2011). These observations suggest that Slik could be activating Stat92E via insulin signaling. Consistent with this, we observed a reduction in activated Akt1 in *slik* deficient embryos despite elevated total Akt1 protein (Figure 5E). A reduction in insulin signaling may in fact explain the longevity of $slik^{1}$ mutant larvae (Hipfner and Cohen, 2003). Raf interaction has been suggested to bridge Slik to the MAPK proliferation branch of cell survival signaling (Hipfner and Cohen, 2003), which our data support, as we find that *slik*-deficient embryos exhibit defects in ERK activation (Figure S5D). Despite a non-essential role for *slik* in embryogenesis, our examination of correlative

phosphorylation during this early stage illuminated Slik function, highlighting the power of our approach.

An examination of Wee-dependent phosphorylation

We chose to more closely examine the phosphoproteomic profile of RNAi-derived *wee* kinase-deficient embryos since their phenotype mirrored that reported for mutant *wee* embryos (Price et al., 2000). Wee, Cdk1 and Aurora, operate in a regulatory kinase cascade to control nuclear divisions in the early embryo. Phosphorylation and activation of Aurora by Cdk1 is inhibited by Wee and delays entry into mitosis. Wee inhibits Cdk1 by phosphorylating a conserved Tyrosine (Tyr15), located in the ATP binding pocket (Campbell et al., 1995; Stumpff et al., 2004). We therefore expected Cdk1 and Aurora to be hyperactive in the absence of Wee. Indeed we find motif enrichment (Figure 6A) among upregulated phosphosites in *wee*-deficient embryos that resembles Cdk and Aurora kinase consensus motifs (Cdk1: pS/T-P-X-K/R; pS/T-P-X-X-K and Aurora: R-R/K-pS/T; R/K-X-pS/T; R-R/K-X-pS/T) (Alexander et al., 2011). Accordingly, we consistently observed less TMT reporter ion signal proportionate to levels of Cdk1 Tyr15 phosphopeptides in *wee*-deficient embryos, implying Cdk1 hyperactivity in this context (Figure 6B). We corroborated this observation by immunoblotting with a Cdk1-pTyr15 antibody (Figure S6A). Significantly, we identified altered phosphorylation on half of those fly proteins whose orthologous yeast counterparts were identified as Cdk substrates (Figure 6C) (Holt et al., 2009). Aurora is also hyperactive in *wee*-deficient embryos, reflected by the upregulation in phosphorylation of characterized targets: Kinesin-like protein at 10A (Klp10A pSer210: 2.5-fold), Inner centromere protein (Incenp pSer163: 1.5-fold and pSer164: 3-fold), and Histone H3 (HH3 pSer10: 15-fold; pSer28: 7-fold) (Adams et al., 2001; Jang et al., 2009; Kang et al., 2001). We verified HH3 phospho-alterations in *wee* deficient embryos by immunoblotting (Figure S6A). Surprisingly, half of the upregulated phosphosites we identified in *wee* kinase-deficient embryos reside within sequence recognized by Cdk1 or downstream Aurora kinase (Figure 6D). This observation highlights the utility of phosphoproteomic signatures to reveal genetic epistasis. We also find enrichment for specific Gene Ontology categories for those phosphoproteins regulated by Wee (Figure 6E). As anticipated, we observed enrichment for cell cycle classified factors, particularly those with mitotic specific functions such as nuclear migration, spindle organization and chromosome segregation. Intriguingly, proteins with roles in chromatin assembly are overrepresented in our list of upregulated phosphoproteins in *wee*-deficient embryos. This is interesting given the reported hypo-condensation of mitotic chromatin in *wee* null embryos (Stumpff et al., 2004). Motif enrichment among downregulated phosphorylations is illustrated (Figure S6B). Another indirect consequence of *wee* knockdown is the upregulation of Stat92E phosphorylation at Tyr711 in *wee*-deficient embryos (Table S5A). Cdk1 has been shown to regulate Stat92E phosphorylation at Tyr711 in cells (Baeg et al., 2005) and indeed we detect elevated Y711-encompassing Stat92E phosphopeptides in *wee*-deficient embryos that cannot be attributed to increased Stat92E levels (Figure S5B).

Wee functions as a conserved tyrosine kinase (Campbell et al., 1995; McGowan and Russell, 1993), ergo we inquired as to whether any phosphoproteins for which tyrosine

phosphorylation was reduced in *wee* deficient embryos are in fact direct Wee targets. We cloned and tagged eight genes for expression in *D. melanogaster* cells, which were selected based on reduced phosphorylation (> 1.5 fold) of the corresponding protein in *wee*-deficient embryos. Of these, we observed HA-tagged Wee in immunoprecipitates of FLAG-tagged Stonewall (Stwl: lane 6, Figure 7A). In the reciprocal direction, we detected FLAG-tagged Klp10A, CG13605, Stwl, and Polychaetoid (Pyd) in immunoprecipitates of HA-Wee (Figure S6D). Consistent with our observations Pyd was previously identified in Wee-FLAG-HA immune complexes (Guruharsha et al., 2011).

We decided to focus on the nuclear protein Stwl since the myb/SANT (Swi3, Ada2, N-CoR, TFIIB)-like domain it possesses has been found to influence histone modifications by modulating chromatin structure (Boyer et al., 2004) and *wee* mutant embryos have reported defects in chromatin condensation (Stumpff et al., 2004). Like other heterochromatin regulators, Stwl influences position effect variegation and HH3 methylation *in vivo* (Maines et al., 2007; Yi et al., 2009). We found that phosphopeptides encompassing Stwl Tyr305 were reduced in *wee*-deficient embryos (Figure 6F), despite total Stwl levels being elevated (lane 2 versus lane 1: Figure 7D). These alterations in protein cannot be attributed to mRNA transcript stability (Figure S6C). Based on our observations that *wee* is required for Stwl-Tyr305 phosphorylation, we examined the effects of *wee* overexpression on Tyr phosphorylation of Stwl in cells. Tyr phosphorylation of Stwl is elevated in cells overexpressing *wee*, based on phospho-Tyr immunoprecipitation and detection by immunoblotting (Figure 7B). To ask if Wee can directly phosphorylate Stwl, we generated His-tagged Stwl-fusion proteins for *in vitro* kinase assays. We incubated purified His-Stwl fragments with human WEE1 (38% identity, 53% similarity to *D. melanogaster* Wee). WEE1 phosphorylated Stwl at multiple sites recognized by a phospho-Tyr antibody, including fragments encompassing Tyr305 (Figure 7C, lanes 1 and 2). Interestingly, the BESS domain-containing fragment consistently inhibited WEE1 kinase activity as indicated by reduced WEE1 autophosphorylation, both as a His (Figure 7C) and GST tagged fusion protein (data not shown). The BESS motif is likely the region that interacts with Wee given that this domain facilitates protein-protein interactions (Bhaskar and Courey, 2002) and is often found together with the myb/SANT domain. The BESS motif of Suppressor of variegation 3–7 (Su(var)3–7) is required for its chromatin silencing properties (Jaquet et al., 2006). Like Su(var)3–7, Stwl influences trimethylation of HH3 at Lys9, in addition to Lys27 at larval stages (Yi et al., 2009). We detected no obvious reduction in these repressive marks in *stwl*-depleted embryos. Rather, we observed alterations in trimethylated Lys4 of HH3 - an activation mark (Figure 7E). Consistent with a role for Wee in inhibiting Stwl activity, HH3 trimethyl Lys4 marks are elevated in *wee*-deficient embryos (Figure 7E). Effects of *wee* knockdown on Lys4 methylation in later stage 2–4 hour embryos was confounded by the inability of *wee* deficient embryos to transit the MBT (data not shown). Based on our observations, we propose that Wee inhibits the ability of Stwl to modulate histone methylation prior to the MBT, halting the activation of zygotic transcription to regulate the timing of transit through the MBT.

Discussion

A resource to study protein kinases and phosphatases in early embryos

We generated a validated collection of transgenic *D. melanogaster* shRNA lines targeting protein kinases and phosphatases maternally deposited in embryos. The collection permits the examination of zygotic lethal gene perturbations, without the effort of germline clone derivation. Multiple lines of evidence support that the embryonic phenotypes generated by our collection are indeed a result of shRNA on-targeting: 1) near identical qualitative phenotypes generated by two unique shRNAs targeting the same gene for the 15% of the collection we tested; 2) abolition of shRNA-induced phenotypes by substitution of three nucleotides (C911s) precluding on-target binding; 3) the high degree of overlap between our shRNA-derived phenotypes and literature reported mutant embryo and germline clone-derived embryo phenotypes; and 4) our general inability to accredit specific shRNA phenotypes to candidate OTEs, derived from proteomics and partial complementarity matching.

A general method to predict kinase motifs and targets

Using our shRNA collection, we performed quantitative phosphoproteome assessments of genetically compromised animals. An advantage of our gene knockdown strategy over gene knockout is that we restrict RNAi to the germline: since germline development is dispensable for organismal development our RNAi method likely avoids major adaptation and compensation due to effects on the viability of the animal, like that seen for example with yeast deletion mutants (Bodenmiller et al., 2010; Teng et al., 2013). Additionally, the modest amount of transcription in early stage embryos further minimizes the possibility of compensation at the transcriptional level, although non-transcriptional compensation is a possibility. Conceivably, by comparing genetic knockout to incomplete depletion by RNAi-mediated knockdown, one could identify compensatory rewiring events. From phosphoproteomic profiling of kinase-deficient embryos, we identified altered phosphorylation of characterized substrates of depleted kinases, and generated an extensive list of candidate substrates of the depleted kinase and altered phosphoproteins targeted by downstream kinases. A challenge will be to distinguish between primary and secondary targets. It is difficult to evaluate the number of primary targets per kinase since this will depend on multiple factors including the function of the kinase, its expression level, localization, and connectivity with other proteins. Indeed, studies from yeast and mammalian kinases have illustrated that the number of substrates for any one kinase can range from hundreds to only a few (Ubersax and Ferrell, 2007). Thus, we expect variability in the number of substrates depending on the analyzed kinase. Further, biologically meaningful alterations in phosphorylation may have been missed in our analyses, given the limitations of current mass spectrometry technology. We illustrate however that current instrumentation can be used to identify known and predicted targets relevant to the function of the perturbed kinase (*e.g.* Stwl is a direct target of Wee kinase), and so despite perhaps only scratching the surface, we have generated biologically pertinent information. Additional information such as *in vitro* kinase activity towards a substrate, protein-protein interaction, and functional assays are necessary of course to infer a direct kinase-substrate relationship (Sopko and Andrews, 2008). Undoubtedly, extension of our methodology will

be effective for systematically mapping substrates to culpable kinases, and pinpoint critical phosphosites important for substrate function.

Correlation and anti-correlation: an application for network analysis

Our correlative analysis examining coordination between alterations in phosphosite pairs among kinase-deficient profiles uncovered signaling mechanisms. We demonstrate how a role for Slik kinase in regulating the transcription factor Stat92E could be predicted from correlative phosphorylation of these two proteins. The predictive power of this approach could be extended by knowing if specific phosphorylation events serve activating or inhibitory functions and by superimposing kinase consensus motifs. Most excitingly, our analysis demonstrates how functional phosphorylation might be uncovered in any phosphoproteomic data using simple correlative principles. Notably, predictions for any particular kinase can be made indirectly from its detection in varying genetic contexts, with no requirement for direct modulation of the queried kinase. The data we generated from embryos will complement orthogonal datasets such as kinase consensus motif and protein-protein interaction data derived from, for example, peptide and protein chip assays, co-affinity purifications, and yeast two-hybrid assays. Further, phosphosite correlation information could be integrated with large-scale RNAi phenotype data in order to predict whether phosphorylation of a target by a specific kinase serves an activating or inhibiting function.

Perspective

Given that key signaling pathways and kinases implicated in human disease are conserved in *Drosophila* (Rubin et al., 2000), the insight gained from our kinase-deficient phosphoproteomic signatures constitutes an important step towards understanding the kinome network. Going forward we anticipate that phosphoproteomic assessment of other post-translational modifications and more complex genotypes, using combinatorial knockdown (two shRNAs) or knockdown in combination with transgene overexpression or gain-of-function mutations, will appreciably illuminate our ability to decipher signaling mechanisms. In this way global proteomic analyses could map pathways, but also reveal critical nodes in signaling that may partially or completely overcome mutations resulting in pathway hyperactivity. Alternatively, phosphoproteomic assessment of a sensitized kinase mutant in the context of a substrate gain-of-function could expose altered signaling mechanisms contributing to compromised viability (Sopko et al., 2006). Finally, genetic combinations would mimic more natural scenarios in terms of genetic heterogeneity contributing to susceptibility to disease and by mapping contextual phosphorylation improve upon our ability to predict and target essential signaling nodes.

Experimental Procedures

Detailed methods are available in Extended Experimental Procedures. Mass spectrometric sample preparation is further described in the Protocol.

Transgenic shRNA line generation

Twenty-one base pair shRNAs were cloned into VALIUM series vectors and injected into embryos for targeted phiC31-mediated integration at genomic attP landing sites on the second or third chromosome as previously described (Ni et al., 2011). All transgenic lines were sequenced to confirm identity of the shRNA and miR-1 scaffold.

Protein kinase or phosphatase deficient embryo derivation

Females heterozygous for the UAS-shRNA and either MTD-Gal4 (Petrella et al., 2007), expressing three versions of Gal4 sequentially throughout oogenesis, or tub-Gal4, a line expressing Gal4 from a maternal tubulin promoter at two insertion sites during mid and late oogenesis (Staller et al., 2013), were crossed to UAS-shRNA males to recover fertilized embryos.

RNA isolation, reverse transcription, and RT-qPCR

RNA was isolated by guanidinium thiocyanate-phenol-chloroform extraction using TRIzol (Life Technologies) and glass bead based cell disruption. Genomic DNA was eliminated by incubation with DNAse (Qiagen) and samples processed for cleanup with an RNeasy MinElute Cleanup Kit (Qiagen). One microgram of purified RNA was incubated with a mix of oligo (dT) and random hexamer primers and iScript reverse transcriptase (iScript cDNA Synthesis Kit, Bio-Rad) for cDNA synthesis. cDNA was used as template for amplification with validated primers in iQ SYBR Green Supermix with a CFX96 Real-Time PCR detection system (Bio-Rad). Query gene expression was relative to a control sample, normalized to the expression of three reference genes: *ribosomal protein L32*, *alpha-tubulin*, and either *nuclear fallout* or *Gapdh1*, using the ΔΔC(t) analysis method.

Maternal phenotype derivation

Hatch rate was calculated from counting embryos twenty-four hours after deposition. For genotypes with defective hatching, cuticles prepared in Hoyer's mounting media were imaged with a Zeiss AxioCam HRC Camera mounted on a Zeiss Axiophot microscope.

Co-immunoprecipitation and immunoblotting

Lysates were subjected to immunoprecipitation using the indicated antibodies, and samples were subjected to SDS-PAGE followed by immunoblotting.

Quantitative Phosphoproteomics

Embryos lysed in 8 M urea were digested with trypsin, peptides chemically labeled with one of six TMT Isobaric Mass Tags (Thermo Scientific), separated into 12 fractions by strong cation exchange (SCX) chromatography, purified with TiO_2 microspheres and analyzed via LC-MS/MS on an Orbitrap Velos Pro mass spectrometer (Thermo Scientific). Peptides were identified by Sequest and filtered to a 1% peptide FDR. Proteins were filtered to achieve a 2% final protein FDR (final peptide FDR near 0.15%). TMT reporter ion intensities for individual phosphopeptides were normalized to the summed reporter ion intensity for each TMT label. The localizations of phosphorylations were assigned using the AScore algorithm.

In vitro kinase assay

In vitro kinase assays were carried out as described (Sopko et al., 2006).

Correlative analysis

A phosphosite matrix was constructed where rows correspond to identified phosphosites and columns to kinase-deficient datasets. Only phosphosites with ≥ 0.58 log2 fold change were distinguished, by values +1 and −1, based on an increase or decrease respectively in levels relative to an shRNA control. All pair-wise combinations of phosphosites were classified as positive or negative correlating based on their change in the same or opposite direction, respectively for each kinase deficient condition. A correlation sign score was determined, considering the number of positive and negative correlations and the total number of kinase-deficient phosphorylation profiles where both phosphosites change.

Supplementary Material

Refer to Web version on PubMed Central for supplementary material.

Acknowledgments

We thank S. Campbell, D. McKearin, and T.T. Su for flies and antibodies. We thank the Transgenic RNAi Project (TRiP) at Harvard Medical School for flies, specifically R. Tao for shRNA plasmid construction, C. Villalta and P. Namgyal for injections, C. Kelley for help with sequencing, A. Housden and A. Miller for help with stock establishment and L. Holderbaum for TRiP database management. We additionally thank the Bloomington Drosophila Stock Center for flies, the Developmental Studies Hybridoma Bank for antibodies, and the Drosophila RNAi Screening Center (Harvard Medical School), particularly Q. Gilly and I. Flockhart for dsRNA amplicons, equipment, and database assistance. We thank H. Kuhn, W. Kim, S. Mohr, and X. Varelas for critical comments on the manuscript. We thank the Perrimon and Gygi labs for helpful suggestions and advice, E. Huttlin in particular. The National Institutes of Health supported this work (5R01DK088718, 5P01CA120964, 5R01GM084947 and 5R01GM067761). R.S. is a Special Fellow of the Leukemia and Lymphoma Society. N.P. is a Howard Hughes Medical Institute investigator.

References

Adams RR, Maiato H, Earnshaw WC, Carmena M. Essential roles of Drosophila inner centromere protein (INCENP) and aurora B in histone H3 phosphorylation, metaphase chromosome alignment, kinetochore disjunction, and chromosome segregation. J Cell Biol. 2001; 153:865–880. [PubMed: 11352945]

Alexander J, Lim D, Joughin BA, Hegemann B, Hutchins JR, Ehrenberger T, Ivins F, Sessa F, Hudecz O, Nigg EA, et al. Spatial exclusivity combined with positive and negative selection of phosphorylation motifs is the basis for context-dependent mitotic signaling. Sci Signal. 2011; 4:ra42. [PubMed: 21712545]

Baeg GH, Zhou R, Perrimon N. Genome-wide RNAi analysis of JAK/STAT signaling components in Drosophila. Genes Dev. 2005; 19:1861–1870. [PubMed: 16055650]

Bhaskar V, Courey AJ. The MADF-BESS domain factor Dip3 potentiates synergistic activation by Dorsal and Twist. Gene. 2002; 299:173–184. [PubMed: 12459265]

Bodenmiller B, Wanka S, Kraft C, Urban J, Campbell D, Pedrioli PG, Gerrits B, Picotti P, Lam H, Vitek O, et al. Phosphoproteomic analysis reveals interconnected system-wide responses to perturbations of kinases and phosphatases in yeast. Sci Signal. 2010; 3:rs4. [PubMed: 21177495]

Boyer LA, Latek RR, Peterson CL. The SANT domain: a unique histone-tail-binding module? Nat Rev Mol Cell Biol. 2004; 5:158–163. [PubMed: 15040448]

Brand AH, Perrimon N. Targeted gene expression as a means of altering cell fates and generating dominant phenotypes. Development. 1993; 118:401–415. [PubMed: 8223268]

Buehler E, Chen YC, Martin S. C911: A bench-level control for sequence specific siRNA off-target effects. PLoS One. 2012; 7:e51942. [PubMed: 23251657]

Bustin SA, Benes V, Garson JA, Hellemans J, Huggett J, Kubista M, Mueller R, Nolan T, Pfaffl MW, Shipley GL, et al. The MIQE guidelines: minimum information for publication of quantitative real-time PCR experiments. Clin Chem. 2009; 55:611–622. [PubMed: 19246619]

Campbell SD, Sprenger F, Edgar BA, O'Farrell PH. Drosophila Wee1 kinase rescues fission yeast from mitotic catastrophe and phosphorylates Drosophila Cdc2 in vitro. Mol Biol Cell. 1995; 6:1333–1347. [PubMed: 8573790]

Chou MF, Schwartz D. Biological sequence motif discovery using motif-x. Curr Protoc Bioinformatics. 2011; Chapter 13(Unit 13):15–24. [PubMed: 21901740]

Chou TB, Perrimon N. The autosomal FLP-DFS technique for generating germline mosaics in Drosophila melanogaster. Genetics. 1996; 144:1673–1679. [PubMed: 8978054]

Davidson G, Wu W, Shen J, Bilic J, Fenger U, Stannek P, Glinka A, Niehrs C. Casein kinase 1 gamma couples Wnt receptor activation to cytoplasmic signal transduction. Nature. 2005; 438:867–872. [PubMed: 16341016]

Glatter T, Schittenhelm RB, Rinner O, Roguska K, Wepf A, Junger MA, Kohler K, Jevtov I, Choi H, Schmidt A, et al. Modularity and hormone sensitivity of the Drosophila melanogaster insulin receptor/target of rapamycin interaction proteome. Mol Syst Biol. 2011; 7:547. [PubMed: 22068330]

Gnad F, Forner F, Zielinska DF, Birney E, Gunawardena J, Mann M. Evolutionary constraints of phosphorylation in eukaryotes, prokaryotes, and mitochondria. Mol Cell Proteomics. 2010; 9:2642–2653. [PubMed: 20688971]

Graveley BR, Brooks AN, Carlson JW, Duff MO, Landolin JM, Yang L, Artieri CG, van Baren MJ, Boley N, Booth BW, et al. The developmental transcriptome of Drosophila melanogaster. Nature. 2011; 471:473–479. [PubMed: 21179090]

Guruharsha KG, Rual JF, Zhai B, Mintseris J, Vaidya P, Vaidya N, Beekman C, Wong C, Rhee DY, Cenaj O, et al. A protein complex network of Drosophila melanogaster. Cell. 2011; 147:690–703. [PubMed: 22036573]

Hipfner DR, Cohen SM. The Drosophila sterile-20 kinase slik controls cell proliferation and apoptosis during imaginal disc development. PLoS Biol. 2003; 1:E35. [PubMed: 14624240]

Holt LJ, Tuch BB, Villen J, Johnson AD, Gygi SP, Morgan DO. Global analysis of Cdk1 substrate phosphorylation sites provides insights into evolution. Science. 2009; 325:1682–1686. [PubMed: 19779198]

Hu Y, Flockhart I, Vinayagam A, Bergwitz C, Berger B, Perrimon N, Mohr SE. An integrative approach to ortholog prediction for disease-focused and other functional studies. BMC bioinformatics. 2011; 12:357. [PubMed: 21880147]

Hu Y, Roesel C, Flockhart I, Perkins L, Perrimon N, Mohr SE. UP-TORR: online tool for accurate and Up-to-Date annotation of RNAi Reagents. Genetics. 2013a; 195:37–45. [PubMed: 23792952]

Hu Y, Sopko R, Foos M, Kelley C, Flockhart I, Ammeux N, Wang X, Perkins L, Perrimon N, Mohr SE. FlyPrimerBank: an online database for Drosophila melanogaster gene expression analysis and knockdown evaluation of RNAi reagents. G3 (Bethesda). 2013b; 3:1607–1616. [PubMed: 23893746]

Hummel T, Attix S, Gunning D, Zipursky SL. Temporal control of glial cell migration in the Drosophila eye requires gilgamesh, hedgehog, and eye specification genes. Neuron. 2002; 33:193–203. [PubMed: 11804568]

Jang CY, Coppinger JA, Seki A, Yates JR 3rd, Fang G. Plk1 and Aurora A regulate the depolymerase activity and the cellular localization of Kif2a. J Cell Sci. 2009; 122:1334–1341. [PubMed: 19351716]

Jaquet Y, Delattre M, Montoya-Burgos J, Spierer A, Spierer P. Conserved domains control heterochromatin localization and silencing properties of SU(VAR)3–7. Chromosoma. 2006; 115:139–150. [PubMed: 16463146]

Kang J, Cheeseman IM, Kallstrom G, Velmurugan S, Barnes G, Chan CS. Functional cooperation of Dam1, Ipl1, and the inner centromere protein (INCENP)-related protein Sli15 during chromosome segregation. J Cell Biol. 2001; 155:763–774. [PubMed: 11724818]

Landry CR, Levy ED, Michnick SW. Weak functional constraints on phosphoproteomes. Trends Genet. 2009; 25:193–197. [PubMed: 19349092]

Maines JZ, Park JK, Williams M, McKearin DM. Stonewalling Drosophila stem cell differentiation by epigenetic controls. Development. 2007; 134:1471–1479. [PubMed: 17344229]

Manning G, Whyte DB, Martinez R, Hunter T, Sudarsanam S. The protein kinase complement of the human genome. Science. 2002; 298:1912–1934. [PubMed: 12471243]

Marguerat S, Schmidt A, Codlin S, Chen W, Aebersold R, Bahler J. Quantitative analysis of fission yeast transcriptomes and proteomes in proliferating and quiescent cells. Cell. 2012; 151:671–683. [PubMed: 23101633]

McGowan CH, Russell P. Human Wee1 kinase inhibits cell division by phosphorylating p34cdc2 exclusively on Tyr15. Embo J. 1993; 12:75–85. [PubMed: 8428596]

Miller ML, Jensen LJ, Diella F, Jorgensen C, Tinti M, Li L, Hsiung M, Parker SA, Bordeaux J, Sicheritz-Ponten T, et al. Linear motif atlas for phosphorylation-dependent signaling. Sci Signal. 2008; 1:ra2. [PubMed: 18765831]

Morrison DK, Murakami MS, Cleghon V. Protein kinases and phosphatases in the Drosophila genome. J Cell Biol. 2000; 150:F57–62. [PubMed: 10908587]

Ni JQ, Zhou R, Czech B, Liu LP, Holderbaum L, Yang-Zhou D, Shim HS, Tao R, Handler D, Karpowicz P, et al. A genome-scale shRNA resource for transgenic RNAi in Drosophila. Nat Methods. 2011; 8:405–407. [PubMed: 21460824]

Perrimon N, Ni JQ, Perkins L. In vivo RNAi: today and tomorrow. Cold Spring Harb Perspect Biol. 2010; 2:a003640. [PubMed: 20534712]

Petrella LN, Smith-Leiker T, Cooley L. The Ovhts polyprotein is cleaved to produce fusome and ring canal proteins required for Drosophila oogenesis. Development. 2007; 134:703–712. [PubMed: 17215303]

Price D, Rabinovitch S, O'Farrell PH, Campbell SD. Drosophila wee1 has an essential role in the nuclear divisions of early embryogenesis. Genetics. 2000; 155:159–166. [PubMed: 10790391]

Rubin GM, Yandell MD, Wortman JR, Gabor Miklos GL, Nelson CR, Hariharan IK, Fortini ME, Li PW, Apweiler R, Fleischmann W, et al. Comparative genomics of the eukaryotes. Science. 2000; 287:2204–2215. [PubMed: 10731134]

Sawka-Verhelle D, Filloux C, Tartare-Deckert S, Mothe I, Van Obberghen E. Identification of Stat 5B as a substrate of the insulin receptor. Eur J Biochem. 1997; 250:411–417. [PubMed: 9428692]

Sharifpoor S, Nguyen Ba AN, Youn JY, van Dyk D, Friesen H, Douglas AC, Kurat CF, Chong YT, Founk K, Moses AM, et al. A quantitative literature-curated gold standard for kinase-substrate pairs. Genome Biol. 2011; 12:R39. [PubMed: 21492431]

Sopko R, Andrews BJ. Linking the kinome and phosphorylome--a comprehensive review of approaches to find kinase targets. Mol Biosyst. 2008; 4:920–933. [PubMed: 18704230]

Sopko R, Huang D, Preston N, Chua G, Papp B, Kafadar K, Snyder M, Oliver SG, Cyert M, Hughes TR, et al. Mapping pathways and phenotypes by systematic gene overexpression. Mol Cell. 2006; 21:319–330. [PubMed: 16455487]

Staller MV, Yan D, Randklev S, Bragdon MD, Wunderlich ZB, Tao R, Perkins LA, Depace AH, Perrimon N. Depleting gene activities in early Drosophila embryos with the "maternal-Gal4-shRNA" system. Genetics. 2013; 193:51–61. [PubMed: 23105012]

Stumpff J, Duncan T, Homola E, Campbell SD, Su TT. Drosophila Wee1 kinase regulates Cdk1 and mitotic entry during embryogenesis. Curr Biol. 2004; 14:2143–2148. [PubMed: 15589158]

Szilagyi Z, Gustafsson CM. Emerging roles of Cdk8 in cell cycle control. Biochim Biophys Acta. 2013; 1829:916–920. [PubMed: 23643644]

Teng X, Dayhoff-Brannigan M, Cheng WC, Gilbert CE, Sing CN, Diny NL, Wheelan SJ, Dunham MJ, Boeke JD, Pineda FJ, et al. Genome-wide Consequences of Deleting Any Single Gene. Mol Cell. 2013

Ubersax JA, Ferrell JE Jr. Mechanisms of specificity in protein phosphorylation. Nat Rev Mol Cell Biol. 2007; 8:530–541. [PubMed: 17585314]

Wu R, Dephoure N, Haas W, Huttlin EL, Zhai B, Sowa ME, Gygi SP. Correct interpretation of comprehensive phosphorylation dynamics requires normalization by protein expression changes. Mol Cell Proteomics. 2011; 10:M111 009654.

Yan D, Neumuller RA, Buckner M, Ayers K, Li H, Hu Y, Yang-Zhou D, Pan L, Wang X, Kelley C, et al. A regulatory network of Drosophila germline stem cell self-renewal. Dev Cell. 2014; 28:459–473. [PubMed: 24576427]

Yan R, Small S, Desplan C, Dearolf CR, Darnell JE Jr. Identification of a Stat gene that functions in Drosophila development. Cell. 1996; 84:421–430. [PubMed: 8608596]

Yi X, de Vries HI, Siudeja K, Rana A, Lemstra W, Brunsting JF, Kok RM, Smulders YM, Schaefer M, Dijk F, et al. Stwl modifies chromatin compaction and is required to maintain DNA integrity in the presence of perturbed DNA replication. Mol Biol Cell. 2009; 20:983–994. [PubMed: 19056684]

Zhang Y, Liu Y, Li X, Gao W, Zhang W, Guan Q, Jiang J, Frank SJ, Wang X. Effects of insulin and IGF-I on growth hormone- induced STAT5 activation in 3T3-F442A adipocytes. Lipids Health Dis. 2013; 12:56. [PubMed: 23631823]

Highlights

- Transgenic RNAi for knockdown of maternal *Drosophila* protein kinases and phosphatases
- Phosphoproteome changes in kinase-deficient contexts can prioritize kinase targets
- Correlative phosphorylation among genotypes can enrich for functional phosphosites
- Stwl, a chromatin-modifying phosphoprotein, is a Wee kinase substrate

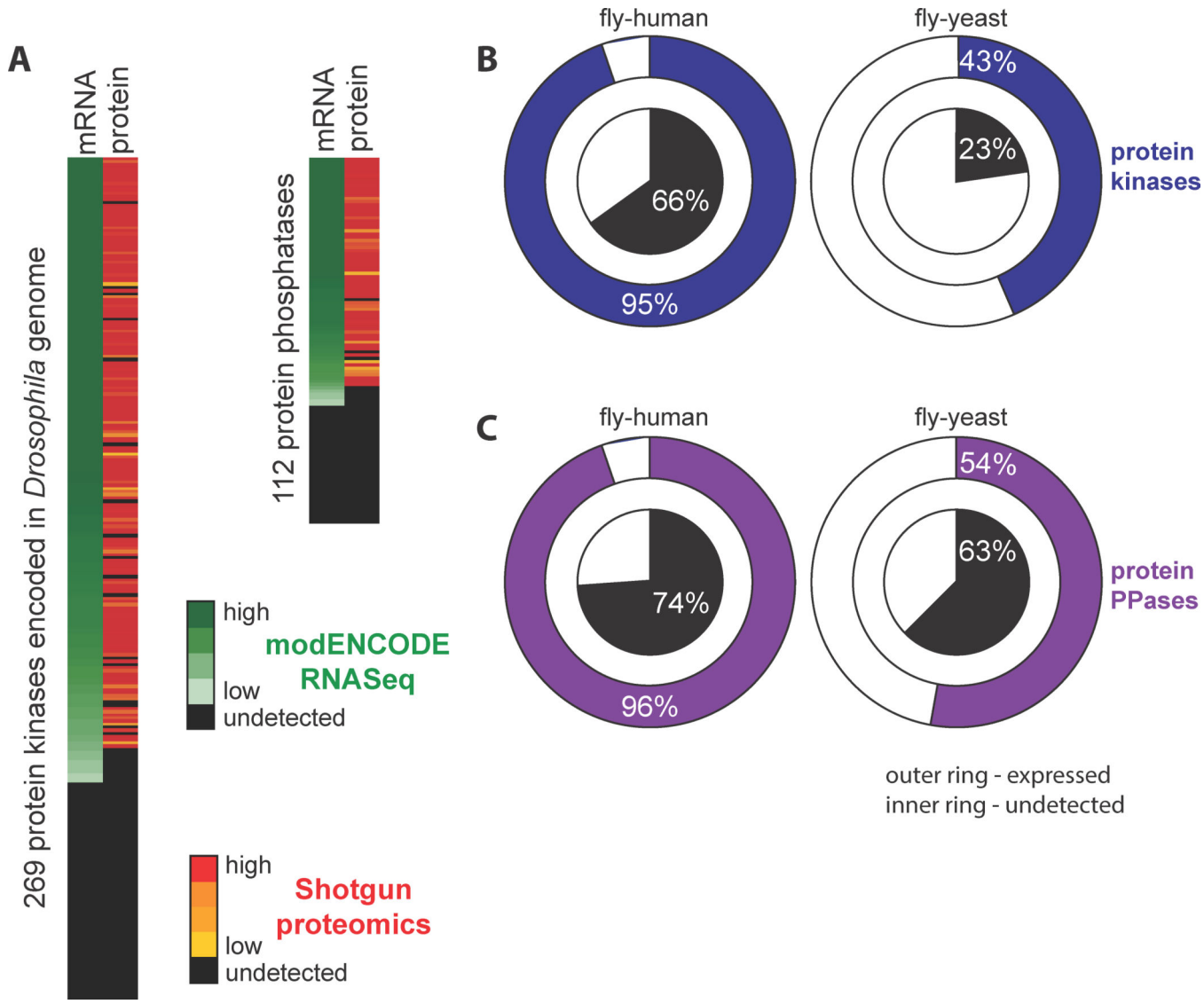

Figure 1. Expression and conservation of protein kinases and protein phosphatases during early *D. melanogaster* embryogenesis

(A) Of 269 *D. melanogaster* protein kinase-encoding genes, 201 were identified by RNA-Seq between 0–4 hours of embryogenesis while 76 of 112 protein phosphatase-encoding transcripts were identified for the same developmental window. Represented is an average RPKM value from two time points comprising stages 1–8. Undetected transcripts are those with less than 3 RPKM. Average RPKM values ranged from high (257: *polo*) to low (3: *btl*, *PVR*, and *CG43143*) for kinases, and from high (327: *mts*) to low (3: *CG565* and *CG16771*) for phosphatases. Corresponding proteins, identified from MS2-based peptide fragmentation were quantified based on label-free peptide MS1 feature intensities from shotgun mass spectrometry for the same developmental time. 172 kinases and 67 phosphatases were quantified. Median signal-to-noise ratios observed across all matching peptides ranged from high (156: Cks30A) to low (5: CG7156) for kinases, and from high (107: Pp2B-14D) to low (6: CG8147 and Ptp4E) for phosphatases.

(B) Conservation of expressed (outer ring) and undetected (inner pie) *D. melanogaster* protein kinases during early embryogenesis (0–4 hours) to human and yeast.
(C) Conservation of expressed (outer ring) and undetected (inner pie) *D. melanogaster* protein phosphatases during early embryogenesis (0–4 hours) to human and yeast. Conservation was considered when 3 or more ortholog predictions tools (DIOPT Score >3) predicted a high confidence ortholog. See also Figure S1.

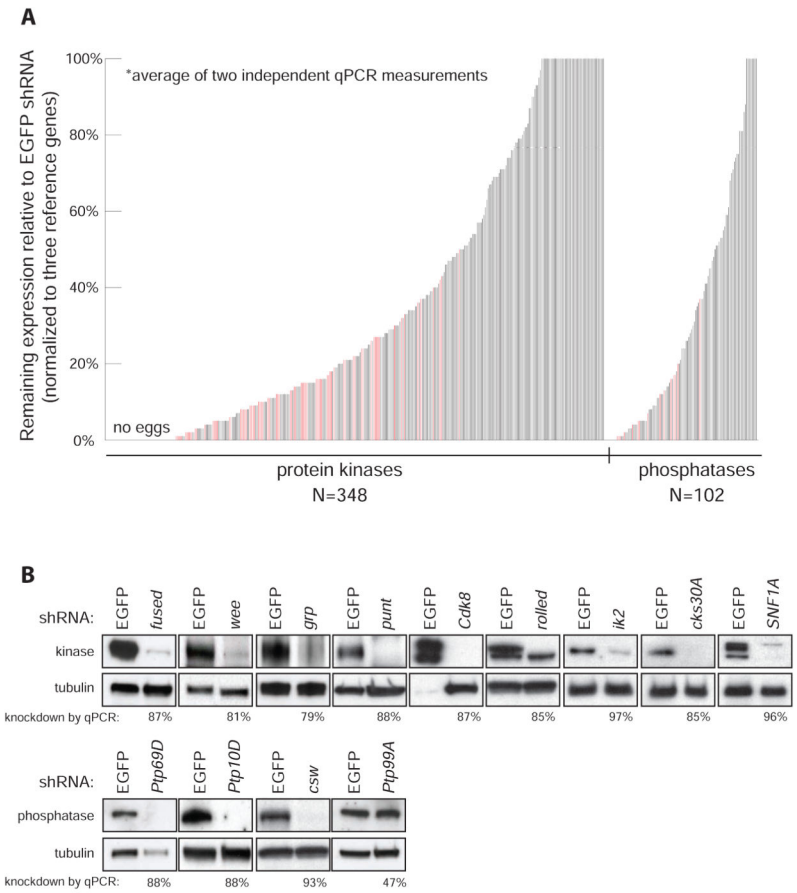

Figure 2. Knockdown efficiency of maternally expressed shRNAs

(A) Plotted is the average remaining transcript level for individual protein kinases and phosphatases targeted by a specific shRNA, relative to an shRNA targeting EGFP, as assessed by RT-qPCR. Three reference genes were used for normalization. Approximately 12% of the lines could not be analyzed since germline knockdown of these genes induced female sterility (no eggs). Indicated in red are lines that generated phenotypes.

(B) Lysate from 0–4 hour embryos was subjected to immunoblotting and levels of the corresponding kinase or phosphatase assessed, relative to tubulin. Indicated below the immunoblots is the extent of knockdown determined by RT-qPCR, achieved for the corresponding shRNA. See also Figure S2.

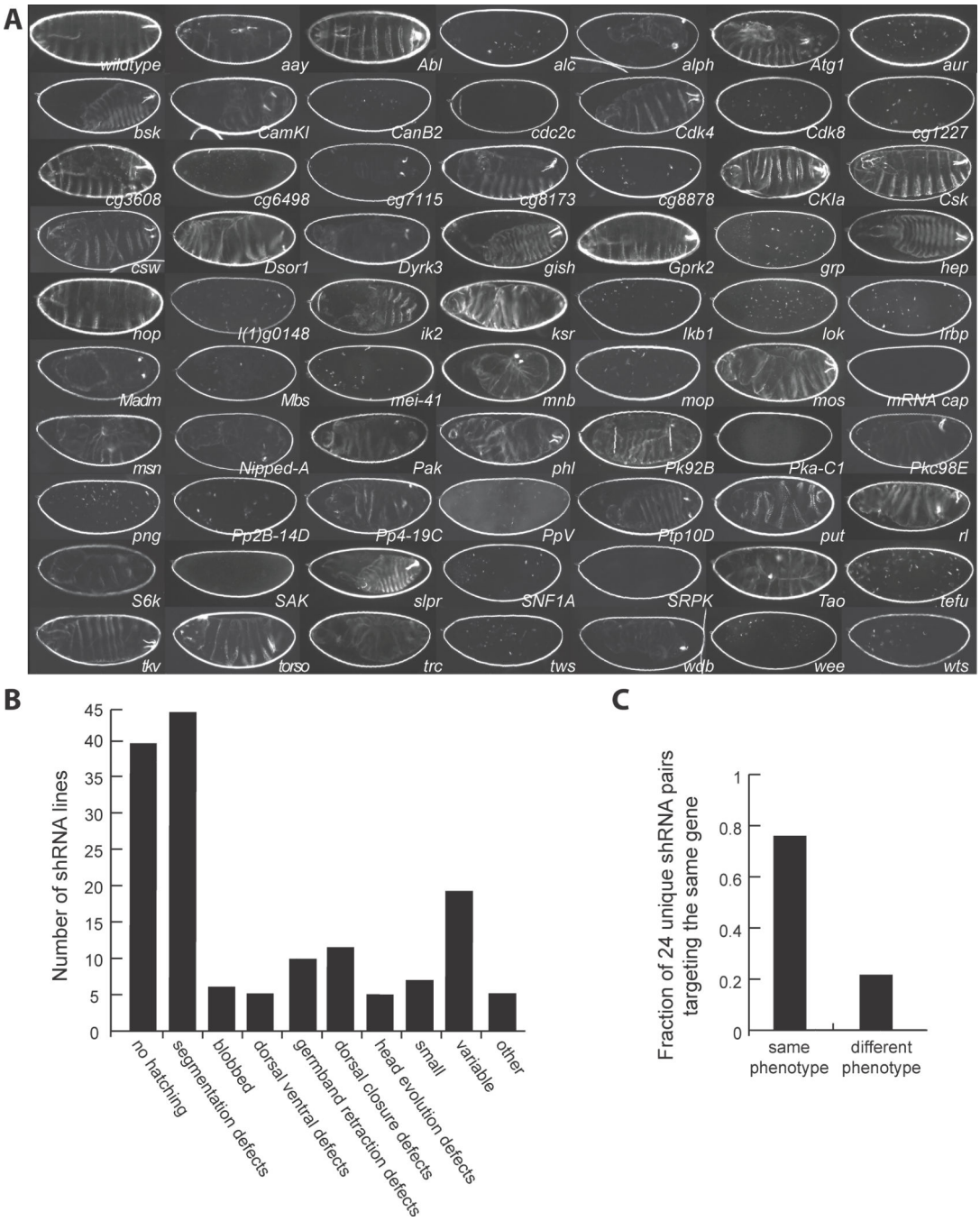

Figure 3. Embryonic phenotypes generated from shRNA-mediated knockdown of maternally contributed protein kinase and phosphatases

(A) Cuticle phenotypes of embryos derived from maternal-Gal4>UAS-shRNA females crossed to UAS-shRNA males. Description of associated phenotypes can be found in Table S2.

(B) Frequency of observed embryonic phenotypes derived from maternal-Gal4/UAS-shRNA females crossed to UAS-shRNA males, from of a total of 450 examined lines.

(C) Twenty-four pairs of shRNAs targeting the same gene and generating >60% knockdown were compared for qualitatively similar embryonic phenotypes. Four of the six cases of a differential phenotype can be explained by degree of knockdown.

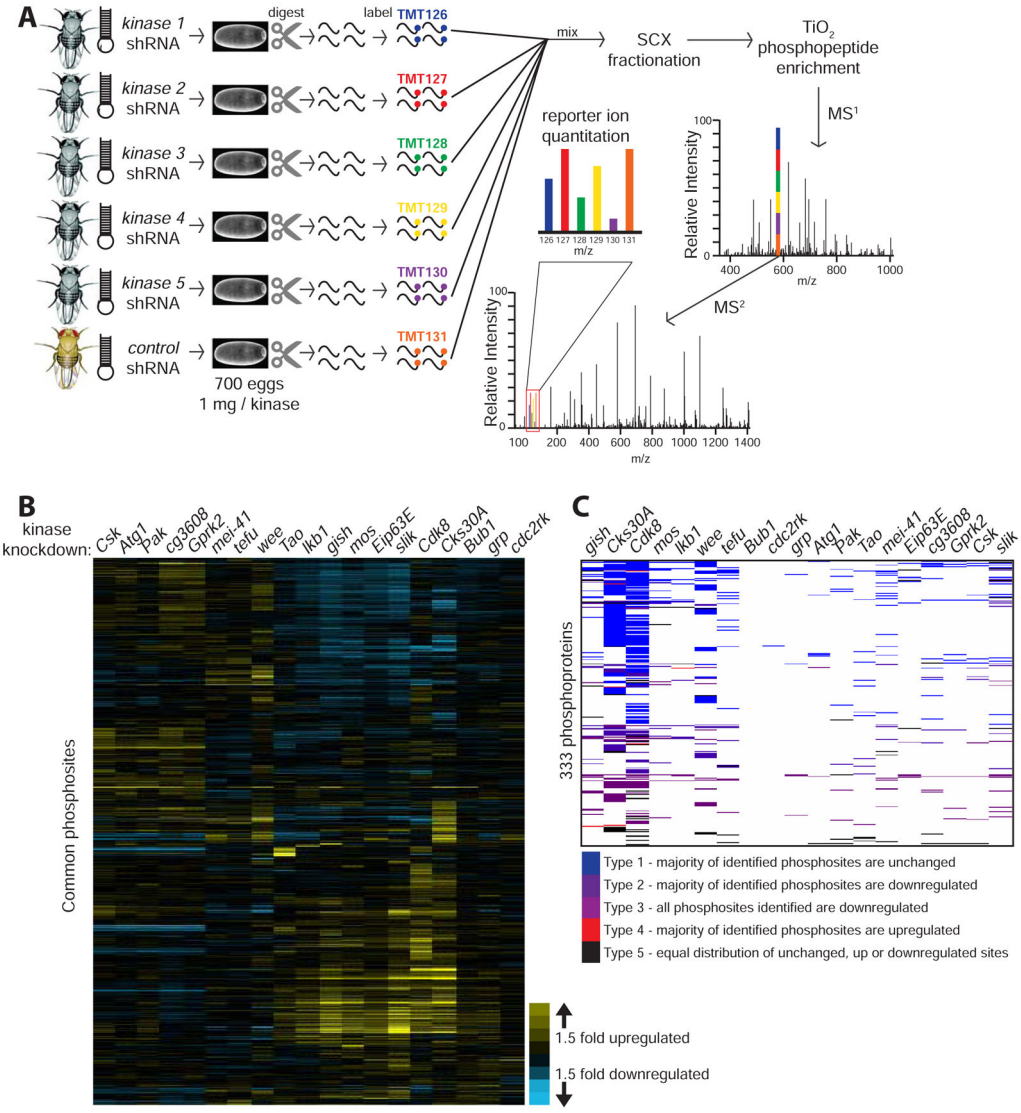

Figure 4. Phosphoprofiles of kinase deficient *D. melanogaster* embryos generated by quantitative mass spectrometry and isobaric labeling with tandem mass tags

(A) Strategy followed to identify differential phosphorylation between kinase shRNA and control shRNA embryos (see Extended Experimental Procedures for details).

(B) Relative phosphosite levels between kinase shRNA and control shRNA embryos. Plotted is the fold change relative to a control shRNA (*white*) for phosphosites found among all experiments. These 1139 unique phosphopeptides meet stringent criteria in terms of isolation specificity and phosphosite assignment (see Experimental Procedures). The hierarchical 2D matrix is clustered based on a correlation distance metric using average linkage. Knockdown efficiencies are: *Cdk8* - 87%; *Cks30A* - 85%; *slik* - 92%; *wee* - 81%; *Tao* - 91%; *mei-41* - 84%; *tefu* - 68%; *lkb1* - 86%; *Atg1* - 92%; *Bub1* - 99%; *grp* - 79%; *cg3608* - 89%; *Gprk2* - 82%; *cdc2rk* - 85%; *gish* - 58%; *mos* - 90%; *Csk* - 90%; *Pak* - 95%; *Eip63E* - 71%.

(C) Phosphoproteins with two or more downregulated phosphosites (> 1.5 fold) were classified into four types based on the directionality of change of the majority of identified phosphosites for the same protein: Type 1 - most identified phosphosites do not change; Type 2 - most identified phosphosites are downregulated; Type 3 - all identified phosphosites are downregulated; Type 4 - most identified phosphosites are upregulated. See also Figure S3 and Figure S4.

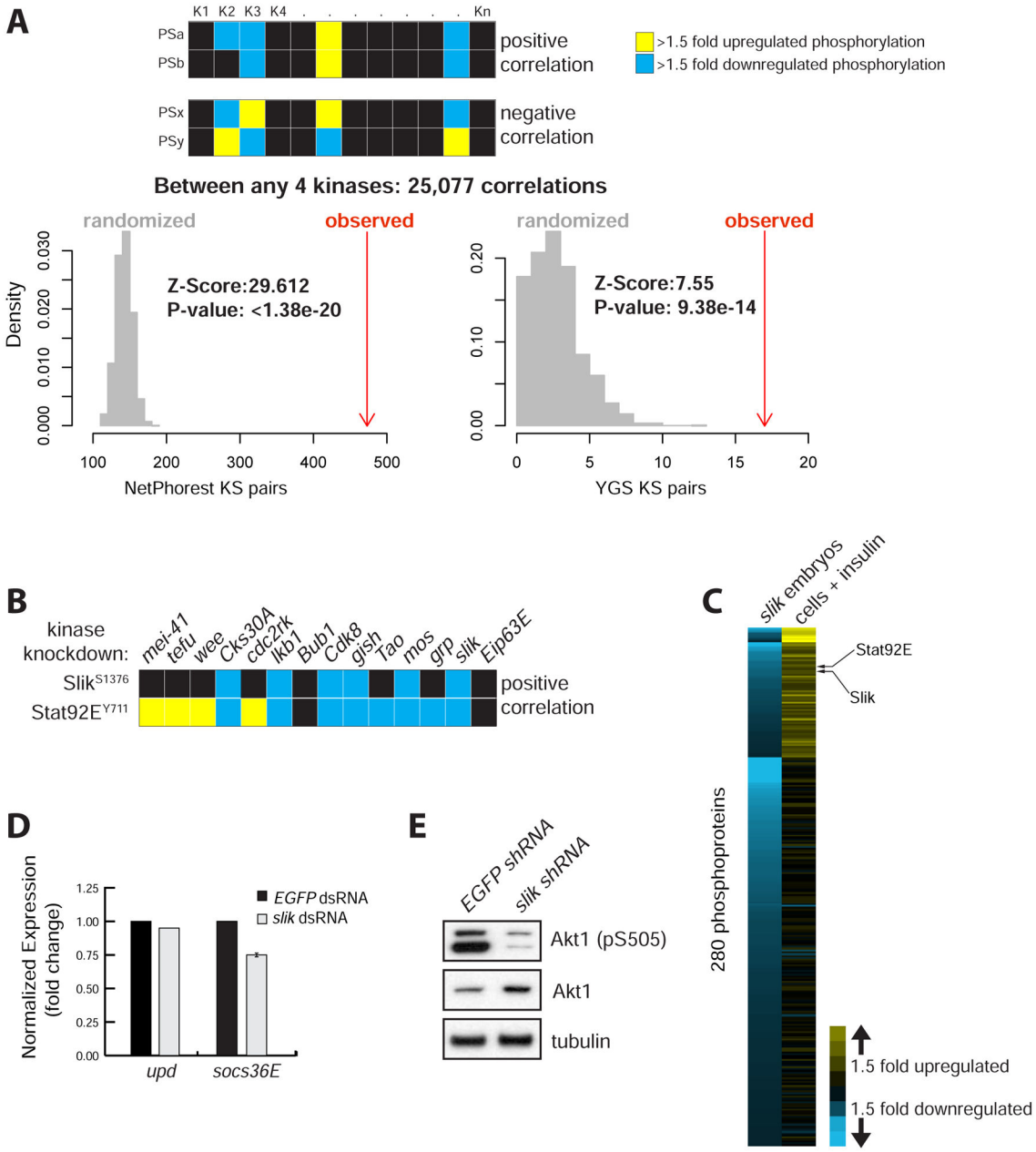

Figure 5. Correlative phosphorylation analysis enriches for kinase-substrate pairs and can reveal signaling mechanisms

(A) Positive and negative correlations in phosphorylation changes (>1.5 fold relative to a control shRNA) between any two phosphosites (PS) were extracted from kinase-deficient phosphorylation profiles. Yeast gold standard (YGS) kinase substrate (KS) pairs (Sharifpoor et al., 2011) were mapped to *D. melanogaster* using DIOPT (Hu et al., 2011). Predicted *D. melanogaster* KS pairs were also predicted based on human kinase phosphorylation motifs from the NetPhorest atlas (Miller et al., 2008). The distribution of expected overlap between KS pairs and 1000 simulated random correlation pairs of the same size, and the overlap is shown in grey. The number of KS pairs observed among all correlation pairs is indicated

(red arrow). Illustrated is the number of pairs when requiring PS correlations among at least four kinase-deficient phosphorylation profiles. Z-Scores and P-values are indicated. See also Figure S5.

(B) For those kinase-deficient embryonic lysates where phosphopeptides encompassing $Slik^{S1376}$ and $Stat^{Y711}$ were detected, we observe a positive correlation in the direction of alteration for these two PS, relative to control.

(C) Comparing common phosphoproteins in *slik*-deficient embryos (exhibiting >1.3 fold downregulation compared to control embryos) to *Drosophila* cells following 10–30 minutes insulin stimulation.

(D) The expression of Stat target genes *upd* and *socs36E* in *Drosophila* cells subjected to *slik* knockdown and stimulated with Upd ligand.

(E) Activated Akt1 (phosphorylation at Ser505) levels in 0–4 hour slik *deficient* embryos. Total Akt1 and tubulin serve as loading controls.

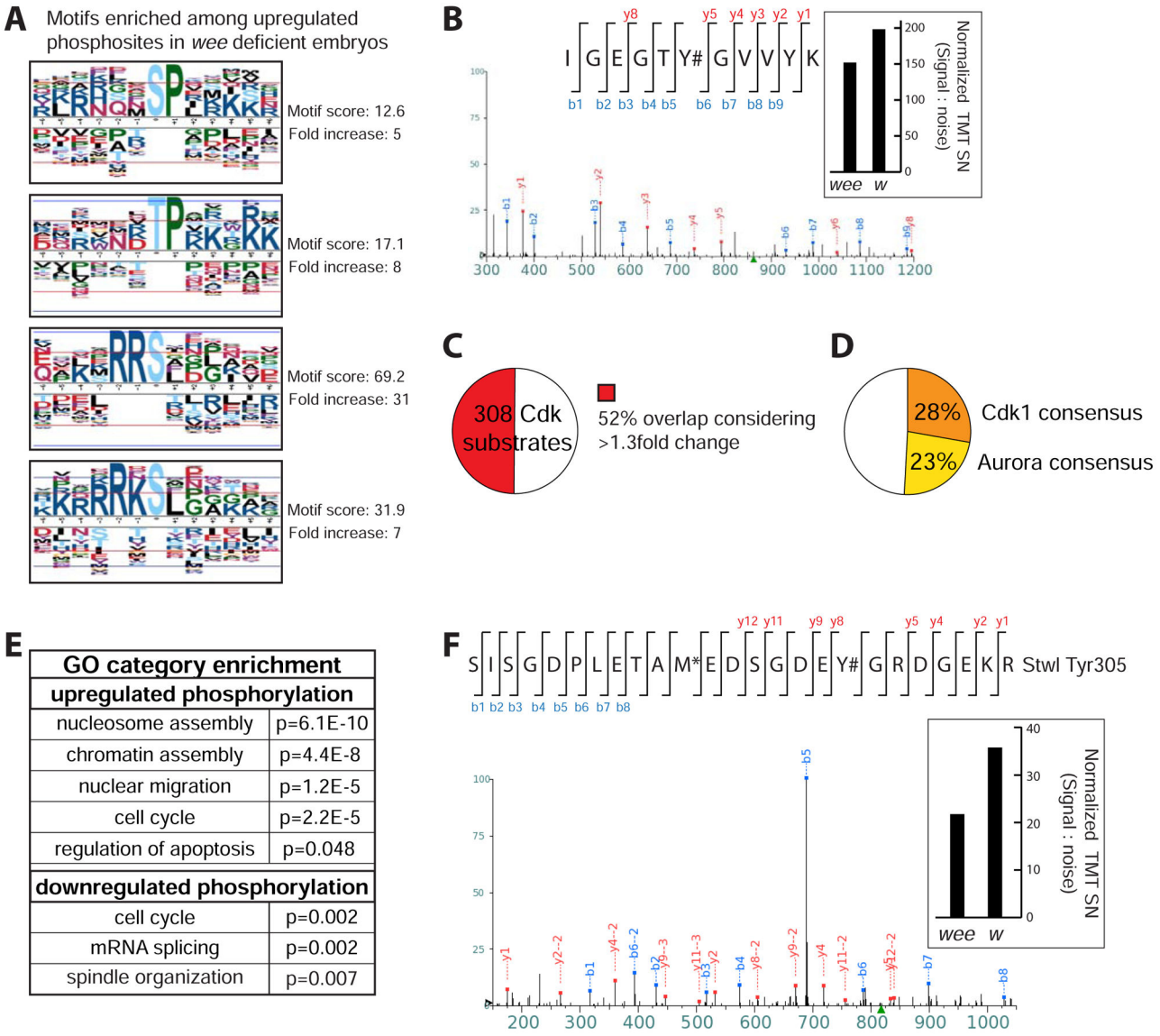

GO category enrichment	
upregulated phosphorylation	
nucleosome assembly	p=6.1E-10
chromatin assembly	p=4.4E-8
nuclear migration	p=1.2E-5
cell cycle	p=2.2E-5
regulation of apoptosis	p=0.048
downregulated phosphorylation	
cell cycle	p=0.002
mRNA splicing	p=0.002
spindle organization	p=0.007

Figure 6. Phosphoproteomic characterization of *wee* deficient embryos

(A) Indicated are motifs encompassing phosphosites that are enriched among phosphosites altered >1.5 fold in *wee*-deficient embryonic lysates relative to control. Motif-X was used to identify motifs (Chou and Schwartz, 2011). The PLogo tool was used to generate motif logos. Favored amino acids at corresponding positions are indicated above the black line while disfavored amino acids are below. "0" indicates the site of phosphorylation.

(B) Levels of a Cdk1 Tyr15 encompassing phosphopeptide in *wee* deficient embryos relative to control embryos (*w*, *white*) as determined by TMT reporter ion signal (right) from the corresponding peptide identified by MS2 fragmentation (left, MS2 spectra). The hashtag indicates the localized site of phosphorylation ($p < 0.05$). Indicated is a representative peptide.

(C) Of 308 phosphoproteins identified as Cdk1 substrates in yeast (Holt et al., 2009), we mapped 120 to fly with a DIOPT Score ≥1. Half of the orthologous *D. melanogaster* counterparts exhibit altered phosphorylation (>1.3 fold) in *wee* deficient embryos.
(D) Approximately half of those phosphosites upregulated >1.3 fold in *wee* deficient kinases can be attributed to Cdk and the downstream kinase Aurora based on kinase consensus motif matching.
(E) Gene Ontology Enrichment among altered phosphoproteins (>1.5 fold) in *wee* shRNA embryos relative to control embryos, identified using the DAVID Functional Annotation Tool.
(F) Levels of a Stwl Tyr305 encompassing phosphopeptide in *wee* deficient embryos relative to control embryos (*w*, *white*) as determined by TMT reporter ion signal (right) from the corresponding peptides identified by MS2 fragmentation (left, MS2 spectra). The hashtag indicates the site of phosphorylation ($p < 0.05$).

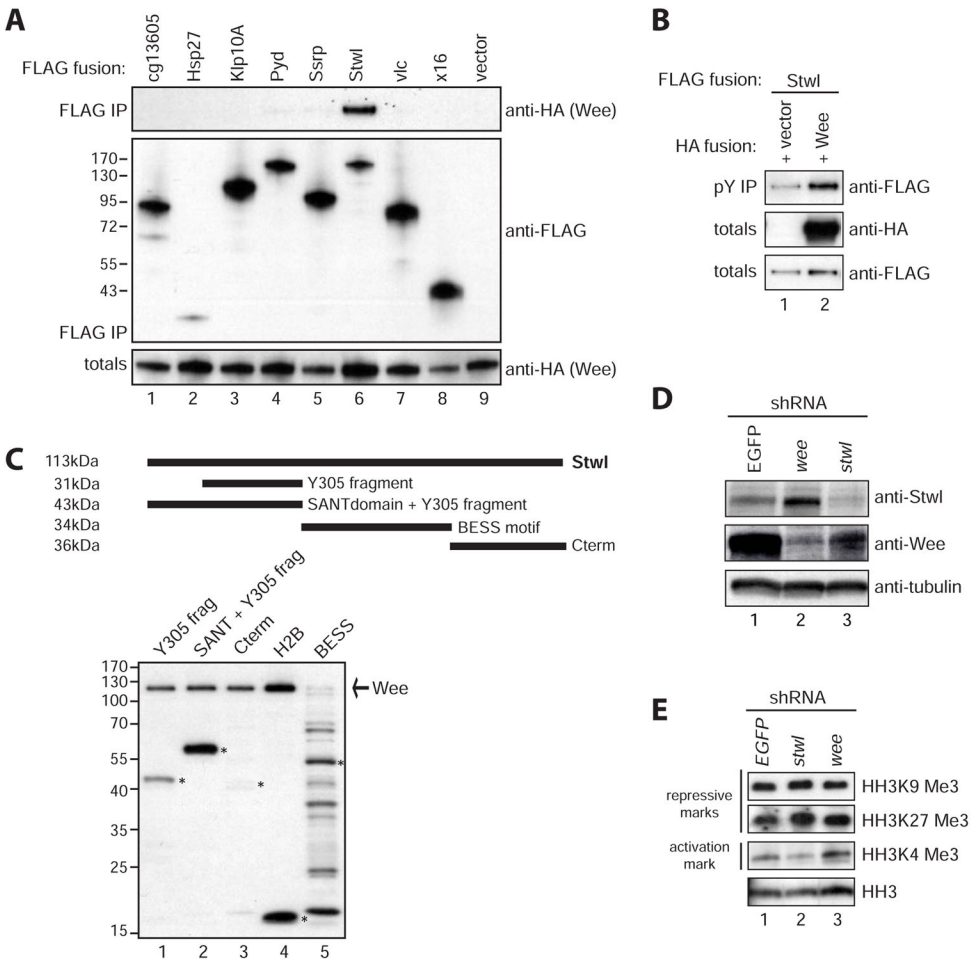

Figure 7. Identification of Stwl as a target of Wee kinase

(A) Lysates from *Drosophila* cells expressing HA-tagged Wee together with 3xFLAG-tagged candidate Wee substrates were subjected to immunoprecipitation with anti-FLAG antibody and analyzed by immunoblotting with the indicated antibodies.

(B) Lysates from *Drosophila* cells expressing HA-tagged Wee together with 3xFLAG-tagged Stwl were subjected to immunoprecipitation with anti-phospho-tyrosine antibody and analyzed by immunoblotting with the indicated antibodies.

(C) Recombinant GST-Stwl fusion proteins were incubated with human WEE1 kinase and radiolabeled ATP and analyzed by SDS-PAGE and autoradiography. Histone H2B serves as a positive control (lane 4). The migration of input proteins is indicated with asterisks. Autophosphorylated WEE1 migrates at 120 kDa.

(D) Lysates from 0–2 hour embryos derived from females expressing shRNAs targeting *wee*, *stwl*, or an EGFP control shRNA were analyzed by immunoblotting with anti-Stwl and anti-Wee antibodies. Immunoblotting with anti-tubulin serves as a loading control.

(E) Lysates from 0–2 hour embryos derived from females expressing shRNAs targeting *wee*, *stwl*, or an EGFP control shRNA were analyzed by immunoblotting with antibodies recognizing different histone H3 (HH3) post-translational modifications.